

# PHYS3033 Lab Report 2:

---

## Neutron Activation Analysis

Damon Binder  
Uni ID: u5591488  
Due Date: 11/05/2015

Neutron activation of indium, vanadium, manganese, tungsten and gold was studied using an americium-beryllium neutron source moderated by polyethylene beads. Using a high-purity germanium detector, the characteristic peaks of the activated isotopes were found, and their energies and intensities calculated. The half-lives of the produced isotopes were then obtained by monitoring the decay of the products. All these results were compared to literature values from the NNDC database and found to be within good agreement. The flux of the neutron source was inferred from the spectra and the thermal neutron capture cross sections, although discrepancies in the calculated value between materials suggested that the neutron source was insufficiently thermalised to apply such an analysis. The use of neutron activation analysis as an analytic technique was tested with an unknown sample.

# Contents

1. Introduction and Background .....	3
1.1 Introduction .....	3
1.2 Irradiation and Radioactive.....	3
1.3 Statistics of Spectra .....	4
2. Experimental Details .....	5
3. Results and Discussion .....	7
3.1 Raw Data .....	7
3.2 Characterising the Detector .....	8
3.3 Peak Finding and Identification.....	12
3.4 Half-Life Calculations.....	18
3.5 Isotope Yields and Neutron Flux .....	21
3.6 Unknown Sample Analysis .....	23
4. Conclusion.....	25
5. Bibliography.....	26
Appendix 1: Python Scripts .....	27
A1.1 Peak finder script .....	27
A1.2 Half-Life Calculator .....	29
Appendix 2: Characteristic Peak Identification .....	31
A2.1 Background Peaks.....	31
A2.2 Sample Peaks .....	34

# 1. Introduction and Background

## 1.1 Introduction

In neutron activation analysis, samples are exposed to a neutron source. The nuclei in the sample can capture the neutron, producing new, and often radioactive nuclei. By monitoring the gamma radiation emitted by the irradiated sample, we can hence determine the composition of a sample.

We exposed various samples to an americium-beryllium neutron source. We then measured the spectra of our irradiated samples to find the characteristic gamma peaks and intensities of these isotopes. For the spectrometry, we used a high-purity germanium detector. Taking multiple measurements allows us to witness the decay of our produced isotopes back to stability, and we can use this to deduce the half lives of the isotopes. *Table 1* lists the samples we irradiated, along with the isotopes produced that could be studied in the lab. The table also lists the isotope half lives, the natural abundance of their parent nuclei, their atomic masses and their thermal neutron cross section. The first two values were taken from Ref. (1), the cross sections were found in Ref. (2), and the atomic masses taken from Ref. (3). We then tested neutron activation analysis by analysing the composition of an unknown sample.

Sample	Isotope Produced	Half Life (s)	Abundance of Parent (%)	Atomic Mass (u)	Thermal Neutron Cross Section (barns)
Gold	<sup>198</sup> Au	232800	100	196.967	98.7
Indium	<sup>116</sup> In	3257	95.71	114.818	194
Manganese	<sup>56</sup> Mn	9284	100	54.938	13.3
Tungsten	<sup>187</sup> W	86400	0.2843	183.84	18.3
Vanadium	<sup>52</sup> V	225	99.750	50.942	5.08

**Table 1:** Samples Used in the Experiment.

## 1.2 Irradiation and Radioactive

In Ref. (4), the activity of an irradiated sample is given as

$$A_0 = \frac{\sigma m \eta \phi \alpha S}{w_A}$$

where  $A_0$  is the activity of the sample immediately after activation ceases,  $\sigma$  is the neutron capture cross section,  $m$  is the sample mass,  $\eta$  is Avogadro's number,  $\phi$  is the neutron flux,  $w_A$  is the molar mass,  $\alpha$  is the fraction of the target isotope in the sample, and  $S = 1 - e^{-\lambda t}$  is the saturation factor. Here  $\lambda$  is the decay constant of the produced isotope, and  $t$  is the time that the sample has been irradiated. Noting that  $N_A = \frac{m \eta \alpha}{w_A}$  is simply the number of target nuclei in the sample, and that  $A_0 = \lambda N_0$ , where  $N_0$  is the total number of produced nuclei, we get the formula

$$N_0 = \frac{\sigma \phi N_A}{\lambda} (1 - e^{-\lambda t}).$$

From this we can see that the amount of produced nuclei depends on the exposure time, but as  $t \rightarrow \infty$  it reaches an equilibrium value of  $\frac{\sigma \phi N_A}{\lambda}$ .

When isotopes decay, the average number of radioactive nuclides left is given by

$$N(t) = N_0 e^{-\lambda t}$$

The decay constant  $\lambda$  is related to the lifetime  $L$  and half-life  $h$  by the formulas:

$$L = \frac{1}{\lambda}, \quad h = \frac{\ln(2)}{\lambda}.$$

### 1.3 Statistics of Spectra

In each channel of a spectrum, the probability of getting  $x$  counts is given by the Poisson distribution

$$P(X = x) = \frac{m^x e^{-m}}{x!}$$

where  $m$  is the mean count rate. In the limit where  $m$  is large, the probability distribution approaches that of a Gaussian with mean  $m$  and uncertainty  $\sqrt{m}$ . However, as noted in Ref. (5), this approximation is only really valid for  $m$  greater than about 100.

Because of the inherent uncertainties in a Poissonian distribution, peaks need to have a sufficiently high count rate to appear over the background. In (5), an estimation of the detection limit is

$$L = 3\sqrt{N_b}$$

where  $N_b$  is the mean background rate.

Here  $L$  is the minimum number of counts required so that the peak is at least  $3\sigma$  larger than the background, 50% of the time. Again this is only applicable if  $N_b$  is sufficiently large. A more detailed discussion of statistical analysis in relation to spectrometry can be found in (5).

## 2. Experimental Details

In the experiment, we first exposed samples to neutron radiation, and then measured the gamma ray spectrum emitted. To irradiate the samples, an americium-beryllium source was used. This was placed 10 cm deep in a bucket filled with polyethylene beads to moderate the neutrons. Samples were placed level to the neutron source, 5 cm from the centre, and left to irradiate for a set time.

Once irradiated, the gamma spectrum of the sample was measured. Since the process of moving the sample from the irradiation bucket to the detector around a minute, the time taken from the removal of the sample from the bucket to the beginning of the first measurement was recorded. The sample was placed in a lead castle with the detector, along with shielding materials. *Figure 1* is a schematic representation of this set up. The sample was placed carefully in the centre of the beryllium window, to maximise the reproducibility of the geometry. A copper shield was used to reduce the intensity of low energy x-rays. To block background radiation, a thick lead shield was used. This was lined with iron to block the lead x-rays.

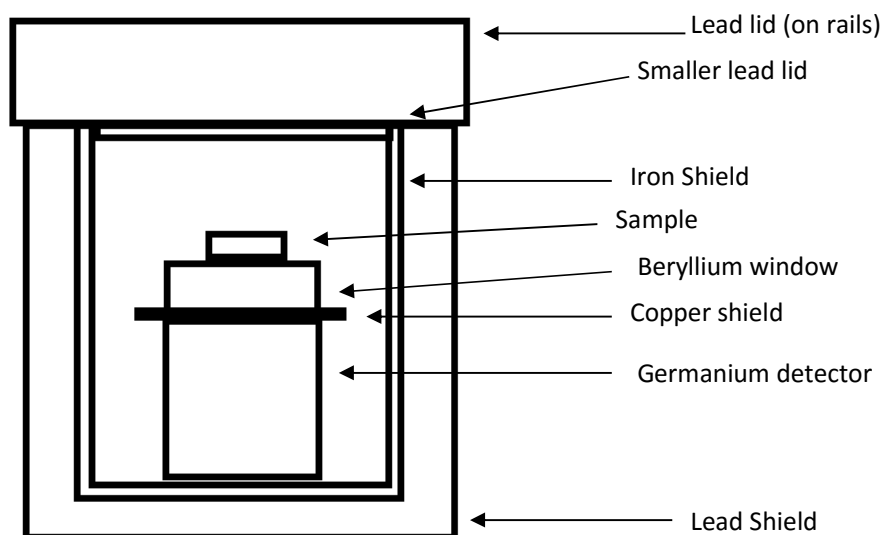


**Figure 1:** Lead Shield Setup.

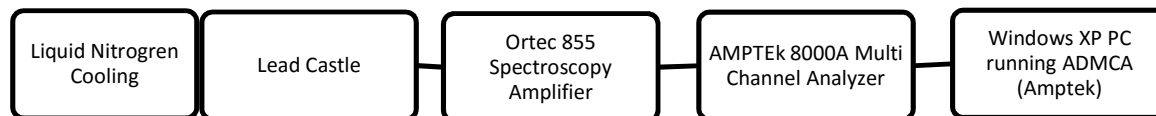


**Figure 2:** Schematic setup of experimental electronics.

In *Figure 2*, the overall spectrometry set-up is shown schematically. The source and detector were placed inside a lead shield. A container of liquid nitrogen was connected to the detector to keep the detector cool. The detector output was processed through the spectroscopy amplifier to amplify the signal, and then the signal was processed using the multi-channel analyser and computer. Using ADMCA allowed us to visualise and analyse the output as a histogram of counts in each region of the

spectrum. For each trial, multiple spectra were taken at different times, to allow us to capture the decay of the produced isotope.

To calibrate the germanium detector, both a  $^{152}\text{Eu}$  and  $^{133}\text{Ba}$  were used. We irradiated Indium, manganese, gold, tungsten, and vanadium samples. To test the effects of irradiation time, indium samples were irradiated for times between half an hour and three hours, in half hour intervals. Since the vanadium sample produced such a weak signal, for some of the vanadium trials the beryllium window and copper shield were removed.

## 3. Results and Discussion

### 3.1 Raw Data

In *Table 2*, the masses of the samples used in the experiment are recorded. As multiple indium samples were used, these have been numbered. Because the unknown sample was covered in aluminium foil, it could not be accurately weighed.

Element	Number	Mass ( $\pm 0.1\text{mg}$ )
Gold		2422.8
Indium	1	6106.0
Indium	2	3409.0
Indium	3	2972.5
Manganese		3452.5
Tungsten		2325.0
Vanadium		4132.8
Unknown	1	

**Table 2:** Samples used in experiment

In *Table 3*, details of the trials we performed are listed. The number of spectra column documents the number of spectra taken. The time that each spectrum was recorded for is given in the “measurement time” column. The “time to begin” column documents the time period between taking the sample out of the irradiation bucket and the beginning of the first measurement. For tungsten and manganese this time was not recorded, although it would have been between one and two minutes. However, as the lifetimes of manganese and tungsten are far larger than this time period, this omission has a negligible impact on our results.

Sample	Irradiation Time ( $\pm 0.02\text{hrs}$ )	Number of Spectra	Measurement Time (s)	Time to begin (s)
Gold	71.4	20	10800	180
Indium (all samples)	0.50	10	600	55
Indium (1)	1.00	6	600	90
Indium (2)	1.50	10	600	71
Indium (1)	2.00	10	600	216
Indium (3)	2.50	10	600	63
Indium (2)	3.00	10	600	60
Manganese	2.43	3	3300	--
Tungsten	26.47	20	7200	--
Vanadium	0.43	6	180	52
Vanadium (no Be window)	1.00	6	180	33
Vanadium (no Be window)	0.98	6	180	32
Unknown	47.83	34	1800	50

**Table 3:** Trials performed in experiment

## 3.2 Characterising the Detector

### Energy Calibration

A  $^{152}\text{Eu}$  source was used to calibrate the energy. We identified the major peaks in the spectrum, and then used the ADMCA software to calculate the centroid of each peak. The results are shown in *Table 4*.

Energy (keV)	Channel
121.78	213.35
244.7	437.60
344.28	619.31
778.9	1412.5
964.08	1750.32
1085.84	1972.52
1112.08	2020.37
1408.01	2560.46

**Table 4:** Peaks and channel of peaks used for the energy calibration

Using ADMCA, we calculated the line of best as

$$E = 4.87982 + 0.548006x$$

where  $E$  is the energy in keV and  $x$  is the channel. This fitting is extremely good, with the largest deviation being 0.038 keV. This implies that our energy calibration is accurate to within about 0.04 keV. The lowest channel we recorded was channel 20, which corresponds to an energy of 15.84keV. Since 4096 channels were used, the last channel corresponds to energy 2249.51keV. However, no counts above channel 3968 were recorded in any of the spectra, with the sharp cut-off suggesting that our setup cannot detect gammas above this channel. Hence the maximum energy detected in this experiment is 2179.37keV. Of course, care is needed to extrapolate the calibration equation below the lowest used peak, 121.78keV, and the highest, 1408keV, since we have no  $^{152}\text{Eu}$  peaks in this region. Studying the peaks of other nuclides will allow us to verify that our calibration still holds in these regions.

### Detector Efficiency

To be able to calculate the amount of radioactive material in a sample, we need to know the relative photopeak efficiency

$$\rho(E) = \frac{\text{counts detected in photopeak}}{\text{total gammas in peak released by source}}.$$

In general this quantity is energy dependent. To calculate this efficiency, we used both our  $^{152}\text{Eu}$  and  $^{133}\text{Ba}$  spectra. First we need to compute the number of decays during the 20 minutes that we detected for. We can compute this quantity,  $R$ , via the formula

$$R = A_0 2^{-\frac{T}{H}} \times 3.7 \times 10^{10}$$

where  $A_0$  is the activity of the source in Curies at calibration,  $T$  is the time since calibration, and  $H$  is the half-life of the source.



The  $^{152}\text{Eu}$  source had  $A_0 = 0.829 \mu\text{Ci}$  with a 5% error in this quantity, a half-life of 13.5 years and was last calibrated in November 2010. We therefore have

$$R_E = 293.4 \pm 0.6 \text{ million counts} \pm 5\% \text{ calibration error}$$

For the  $^{133}\text{Ba}$  source,  $A_0 = 1.01 \mu\text{Ci}$  again with 5% error, a half-life of 10.5 years and was last calibrated in March 2010. This gives us

$$R_B = 342.5 \pm 1.0 \text{ million counts} \pm 5\% \text{ calibration error}$$

The major peaks were identified using the LUND data base (1). Nearby peaks were combined and their intensities summed to find the total intensity of the peak. The number of counts in each of these peaks was calculated by summing over the channels in the peak, and then subtracting away the mean background found in the nearby channels. The results are shown in *Table 5*.

Source	Start Energy (keV)	End Energy (keV)	Counts	Total Intensity (%)	Efficiency (%)
$^{133}\text{Ba}$	29.54	36.12	171210 $\pm$ 521	116.9	0.429
$^{133}\text{Ba}$	52.56	53.65	20985 $\pm$ 215	35.55	2.871
$^{133}\text{Ba}$	76.12	82.15	655465 $\pm$ 879	2.14	5.398 $\pm$ 0.014
$^{133}\text{Ba}$	299.71	305.19	151616 $\pm$ 402	18.34	2.42
$^{133}\text{Ba}$	352.32	358.34	434242 $\pm$ 664	62.05	2.049
$^{152}\text{Eu}$	36.12	46.53	345817 $\pm$ 740	71.19836	1.655
$^{152}\text{Eu}$	117.22	123.8	416712 $\pm$ 694	28.58	4.97 $\pm$ 0.002
$^{152}\text{Eu}$	242.71	246.55	60400 $\pm$ 279	28.58	2.715
$^{152}\text{Eu}$	340.26	346.29	157153 $\pm$ 415	7.583	2.019
$^{152}\text{Eu}$	777.02	781.4	32507 $\pm$ 200	26.536	0.856
$^{152}\text{Eu}$	864.7	871.83	9212 $\pm$ 142	12.942	0.74 $\pm$ 0.003
$^{152}\text{Eu}$	960.05	967.73	29993 $\pm$ 192	4.245	0.694
$^{152}\text{Eu}$	1084.45	1091.03	22879 $\pm$ 166	14.74	0.653
$^{152}\text{Eu}$	1109.11	1114.59	24912 $\pm$ 171	11.934	0.614
$^{152}\text{Eu}$	1404.49	1411.61	30411 $\pm$ 260	13.83	0.493

**Table 5:** Peaks used to calculate energy efficiency. Only uncertainties which were non-zero to the number of digits used are recorded. Note that the efficiency column does not include the 5% error from calibration of the sources.

The energy vs efficiency of the detector is plotted in *Figure 1*. Two different curves were fitted to reflect the different low and high energy behaviours of energy efficiency. Because of the 5% calibration error in the strength of the sources, it is difficult to use points from both spectra, so I decided to first calibrate the high energy curve using the  $^{152}\text{Eu}$  peaks from 120KeV up. A power law of form

$$\rho(E) = 5.1366E^{-0.959}$$

was found to provide a very good fit to the data. The  $R^2$  value of 0.9978 provides a quantitative measure of the goodness of fit; it shows that about 99.8% of the variance in the data can be accounted for by our model. We can now find the relative radioactivity of the  $^{133}\text{Ba}$  source to the  $^{152}\text{Eu}$  source by comparing the predicted efficiency of the 302keV and 356keV barium peaks with the

actual efficiency. Our energy efficiency curve gives values which were 0.887 and 0.898 of the actual values respectively, so the relative radioactivity of the two sources is about 0.893.

Correcting the low barium peaks by this factor, we can then find the low energy behaviour by fitting a curve to the five peaks with energy at or below 120keV. The quadratic

$$\rho(E) = 10^{-3}(-0.009835E^2 + 2.0332E - 52.176)$$

was found to provide a very good fit to these points, with an  $R^2$  value of 0.9941. Note however that this curve gives negative efficiency when the energy is below 30keV, and hence is only valid above this energy. Both efficiency curves are plotted in *Figure 1*. Note that on this curve error bars in the photopeak efficiency are too small to see.

There are two different errors associated with this efficiency. Firstly, we can calculate the variation of the actual photopeak efficiencies from the efficiency predicted by our curves:

$$Err = \frac{Actual\ Efficiency - \rho(E)}{Actual\ Efficiency}.$$

If we do this, then we find that the though most variations are within a few percent of their correct values, the worst photopeak is 9.2% smaller than its predicted efficiency. To get a useful measure of the uncertainty, we note that the standard deviation in the error for the low energy curve is 6.15%, and for the high energy curve is 3.12%. In (5), it is noted that under optimum conditions uncertainties in energy calibration of about 0.5% can be achieved, and that to gain accuracies between 1-2% require many calibration sources and somewhat sophisticated curve fitting. With this in mind, our uncertainties of 6.15% and 3.12% seem reasonable and are acceptable considering our methods. Since the sign and magnitude of the error does not seem to be related to the energy of the peaks otherwise, we should treat this as a random error.

A second source of error is the 5% calibration error in the  $^{152}\text{Eu}$  source. Since this error would uniformly raise or lower the photopeak efficiency regardless of energy by 5%, this error should be treated separately from any random variation, to avoid unnecessarily including the error.

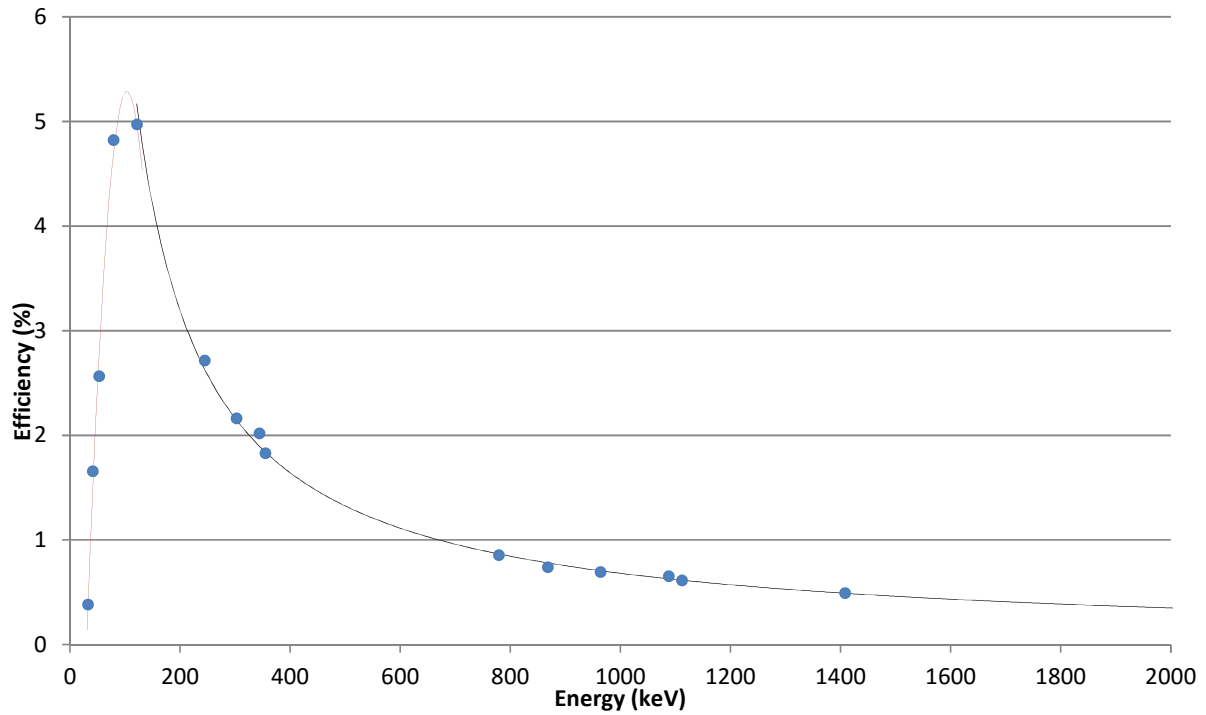


**Figure 3:** Photopeak Efficiency vs Energy. The error bars in the efficiency were too small to be seen on the graph.

## Detector Resolution

In order to evaluate the number of counts in a peak, it is useful to know the energy resolution of our detector. To characterise the resolution we can use the Full Width at Half the Mean (FWHM). This was calculated using a python script was programmed to calculate the FWHM of the major  $^{152}\text{Eu}$  peaks. The program calculated this by performing a background subtraction, and then calculating the mean energy and mean squared energy. The FWHM is then given by

$$\text{FWHM} = 2\sqrt{2 \ln(2)} \sigma = 2\sqrt{2 \ln(2) (\langle E^2 \rangle - \langle E \rangle^2)}$$

The results are shown in *Table 6*. Since the channel width is 0.548 KeV, these values should be taken with a grain of salt. They do however show that if we sum over counts within 2.5 keV of a peak, then we can be confident that this encompasses well over 98% of the total counts in the peak.

Peak Energy (keV)	Full Width at Half the Mean (keV)
121.8343	1.079
244.7944	1.147
344.406	1.227
779.2216	1.473
964.4498	1.576
1112.493	1.587
1408.529	1.796

**Table 6:** FWHM values for major  $^{152}\text{Eu}$  peak.

## 3.3 Peak Finding and Identification

### Methodology

In order to systematically study the energy peaks of our spectra, we need to develop a rigorous method to find these peaks. In a region with a background count rate of  $b$ , we know that the mean number of counts is  $b$ , and the uncertainty in count number is  $\sqrt{b}$ . Hence if we find that the number of counts in the region is actually  $c$ , then the number of standard deviations this is from the mean is

$$\sigma = \frac{c - b}{\sqrt{b}}.$$

For  $\sigma > 2.5$ , Gaussian statistics show that this would occur about 0.62% of the time when no peak is present, and this falls to 0.023% when  $\sigma > 3.5$ . So if we can calculate  $b$  and  $c$  for a given region, we can quickly determine the likelihood of a peak being present.

We still need to choose regions of interest, and then calculate  $b$  and  $c$  for these regions. The simplest method would be to take an individual channel and use the number of counts in this channel as  $c$ . Summing over nearby channels could then be used to calculate the background; in practised, the background was calculated by summing channels between 3 keV and 25 keV from the centre. As discussed in the previous section, the FWHM of peaks is less than 2 keV, so for channels over 3 keV from the centre of a peak, we can be confident that there is almost no contribution from photopeak gamma rays. One difficulty with this method is that peaks are spread over multiple channels. This issue can be solved by searching for a series of channels where  $\sigma$  is persistently large. I chose to include channels where  $\sigma > 1$ . Runs of channels where  $\sigma > 1$  were then treated as a peak and tested for statistical significance.

A more serious issue is that background calculations can be disrupted by peaks lying near the channel. To solve this, we can use a two-step process where the program runs through the spectrum once and identifies channels with counts that are considerably higher than their neighbours. An easy method to determine this is to calculate  $\sigma$  and then exclude points with  $\sigma > 2$ . While this may lower the average background calculated,  $\sigma > 2$  only occurs less than 2.3% of the time for a Poissonian process, and so the effect of this is negligible. In the second step, the program then identifies peaks using the method described in the previous paragraph, but ignores any points which were found to be too far above background in the first step.

Once peaks have been found, we can identify them by comparing their energies to the energies of peaks we expect to see. However, this becomes tedious when there are 60 peaks to identify, so I included in my program a list of peaks I thought I might find in the spectrum. This database includes the spectra of all the isotopes created in the lab from both the NNDC (1) and LUND database (6). A list of commonly found background peaks was also included, using the data in Ref. (7). My program then searches through this list and provides possible identifications for each peak.

I implemented the algorithm using *Python*; the code can be found in *Appendix 1*. For each of the samples irradiated, I summed over all the spectra in order to create the best possible spectrum to identify peaks in. An exception to this is that the Vanadium spectrum only contains two of the three samples, as the third one was badly contaminated by other radioactive material.

## Background Peaks

We begin by identifying the background peaks in our spectrum. Background peaks can be found in all of the spectra, however, the three spectra most useful for this purpose are the background spectrum, the  $^{187}\text{W}$  spectrum and the  $^{198}\text{Au}$  spectrum. While the first spectrum contains only background peaks, it only contains 2.8 hours worth of data, whereas the tungsten and gold spectra contain 40 and 60 hours worth of data respectively. Hence the latter two will contain background peaks that are not visible in the background sample.

While my program is able to find a list of possible sources for each gamma-ray peak, a more detailed analysis is necessary to actually determine the background radiation. Hence to determine the background, I first went through the possible radiation sources, and using the gamma ray intensities calculated for each the peak the total number of decays per hour. If for all the peaks this quantity was consistent, then it seems plausible that the source is present and I can then estimate the number of decays per hour of this source. I can also compare the peaks present to the peaks from the source that are absent. If any major peaks are absent, then it is unlikely that the source is present.

In *Appendix 2*, the peaks present are tabulated and analysed to deduce the source of the background radiation. Although 54 peaks were identified, most of them were from a few sources. *Figure 4* shows the gold spectra, with the major background peaks identified.

Two decay series, the  $^{238}\text{U}$  and  $^{232}\text{Th}$  series, contributed the majority of the background peaks. For the  $^{238}\text{U}$ , all peaks where the mean detection rate was at least 1.6% per decay were detected. In the appendix, the background decay rate for the  $^{238}\text{U}$  series is calculated to be  $4653 \pm 80$  decays per hour. This calculation assumes that the radiation source was concentrated on top of the detector, so that our calculated energy efficiencies could be used. It is more likely that the source is spread throughout the detector container, and the number of decays may therefore be larger. Almost all  $^{232}\text{Th}$  peak peaks with a detection probability over 1% were detected. An important exception to this was the  $^{208}\text{Ti}$  peak, which had a detection probability of 53%, but was not detected. Since this peak is at 84.94 keV, it is probably overshadowed by larger peaks such as the lead x-rays. The background decay rate for the  $^{232}\text{Th}$  series was  $3688 \pm 110$ .

$^{212}\text{Pb}$  and  $^{214}\text{Pb}$  lead x-rays were found between 70 keV and 80 keV. These nuclides are created in the  $^{232}\text{Th}$  and  $^{238}\text{U}$  series respectively, but may also have been present in the lead shielding.

The 1460.82 keV peak from  $^{40}\text{K}$  was also identified. This was amongst the largest of the background peaks, visible on all three of the spectra. The decay rate per hour of  $^{40}\text{K}$  was  $10599 \pm 610$ . The other major primordial nuclide,  $^{235}\text{U}$ , was not detected.

$^{56}\text{Co}$  could plausibly be present in small amounts, but since both its major peaks lie near other background peaks, it is difficult this. The annihilation peak is caused by the annihilation of positrons with electrons, and there are contributions to this curve from all of the nuclides which undergo beta decay. Hence this peak is not particularly useful for determining constituents of the background, but is amongst the most visible peak.

The other peaks present seem to have been caused by activation of either the germanium in the detector, or of the iron shield. Since the size of these peaks depends on the radioactive sources present, a meaningful background rate cannot be calculated for the peaks.

Between 20 and 25keV there is a sharp rise in the number of gamma rays detected. This rise does not have a Gaussian shape, and since our energy efficiency formula breaks down below 30keV, we cannot determine the absolute number of gammas in this region. None of the x-rays from our materials are in this interval. It seems plausible that this rise is not caused by radiation, but is instead an artefact of the detector.

While there were a number of peaks in each of the three spectra that could not be identified, nearly all of them had  $\sigma < 4$  and none of them occurred in more than one of the spectra. Hence, it seems that our list of gamma peaks exhausts the background peaks that are visible in this experiment.

While we have managed to find the nuclear decays responsible for the background peaks, the source of the  $^{238}\text{U}$ ,  $^{232}\text{Th}$ , and  $^{40}\text{K}$  are still not clear. While primordial nuclides are present everywhere, the lead shielding we used should have blocked essentially all of the radiation from outside the castle. This can be tested by noting that the outer layer of lead and the inner layer of iron attenuate gamma rays differently depending on the gamma energy. Since the calculated activities for  $^{238}\text{U}$  and  $^{232}\text{Th}$  show little dependence on energy, the gamma rays have clearly not been attenuated through either of the layers. Since in the  $^{238}\text{U}$  series we detected both  $^{234}\text{Th}$  and  $^{226}\text{Ra}$ , it is also clear that  $^{238}\text{U}$  is present around the detector, and that radon gas entering the detector from outside can only be a small contributor to the lighter nuclei decays in the series.

From these considerations, it seems that the background radiation is from dust near the detector. Using the half-life of the nuclides, we can calculate that there is at least 0.1 mg of uranium, 0.25 mg of thorium, and 1 mg of potassium present around the detectors; this calculation is performed in *Appendix 2*. However, the actual quantity is likely higher depending on the distribution of the dust. For these quantities to be present a hundred grams of average soil would be needed, which is unreasonably high. However, if the dust was from rocks with naturally high uranium and thorium content, then there could be as little as a gram in total of material present.

It is also possible that some of the dust is from the containers used to store our radioactive samples. While we don't have a good enough background to test this, it is clearly a possibility as one of the vanadium spectra we took showed far greater peaks than the others, and so clearly at least one of the containers was contaminated. If this was the case, then the background may vary throughout our measurements.

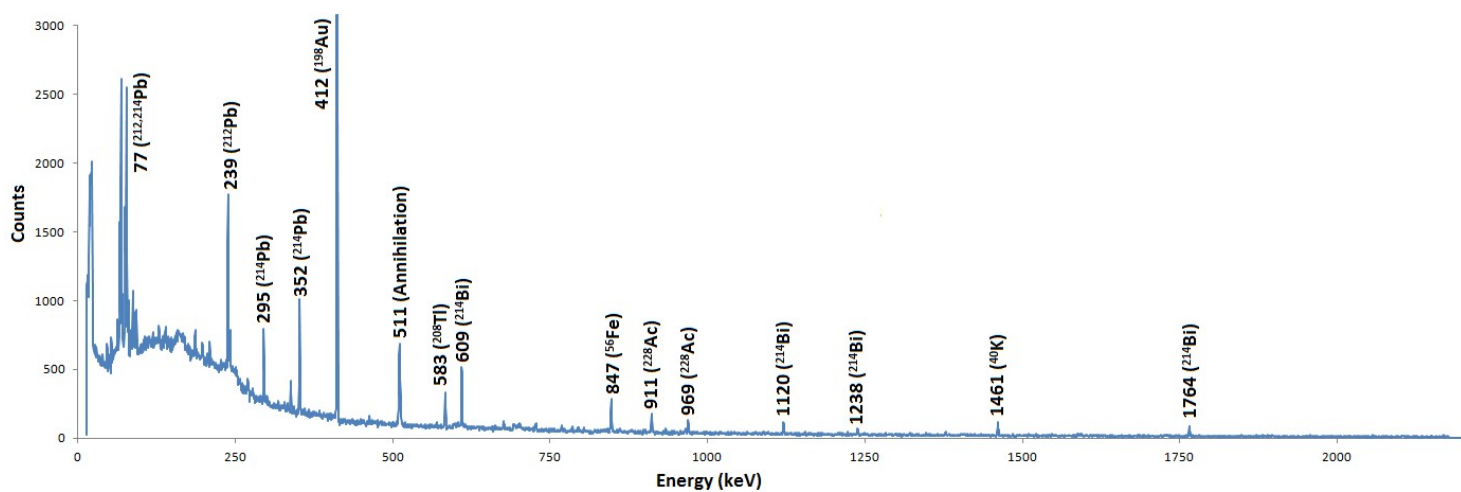
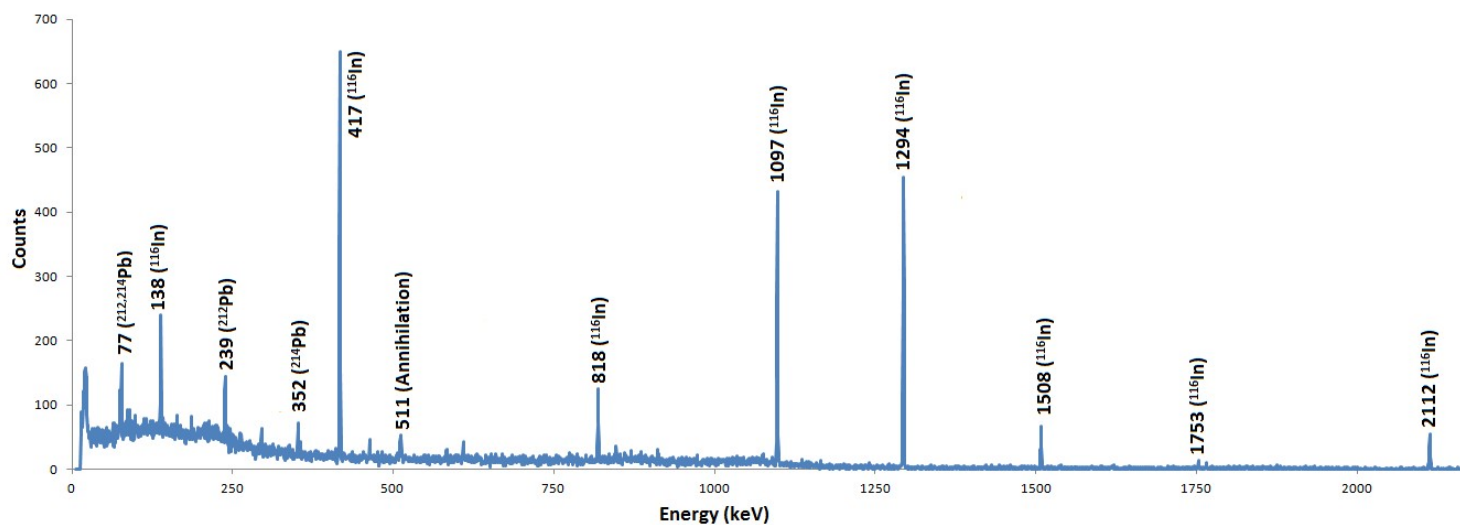


**Figure 4:** Gold spectrum with major peaks identified. Note that the 412  $^{198}\text{Au}$  peak has been cut off; its actual height is 18000.

**Figure 5:** Indium spectrum with the major  $^{116}\text{In}$  and background peaks identified.



## Peaks of Produced Nuclei

Now that we have identified the background peaks, we can analyse the spectra of our produced isotopes without fear of contamination from background peaks. *Figure 4* and *Figure 5* show the spectrum of gold and indium, with the peaks labelled. In *Appendix 2*, I've documented the peaks for these isotopes with intensity greater than 0.1%, and tested whether they were present in our spectra. The peaks which actually occurred and could be discerned over background are given in *Table 7*. In this table, a background count rate of 0 means that no background characteristic peak were found at the same energy. Otherwise, using the background count rates calculated in the previous section, I've calculated the number of counts that have originated from background characteristic peaks which overlap with the peak. To find the true number of counts in the peak which have originated from the nuclide, we can simply subtract the expected number of background counts.

Nuclide	Literature Energy (keV)	Measured Energy (keV)	Literature Intensity (%)	Measured Intensity (%)	Background Counts (per hour)
<sup>198</sup> Au	411.80	411.7	95.62	97.4±4.3	1.13±0.3
<sup>198</sup> Au	675.88	67.0	0.81	0.6±0.1	0
<sup>187</sup> W	59.72		8.35±0.24		
<sup>187</sup> W	61.14		14.3±0.4		
<sup>187</sup> W	Combined	60.0	22.7±0.6	26.6±2.3	8.28±0.1
<sup>187</sup> W	69.31	69.1	3.17±0.09	3.7±0.5	0
<sup>187</sup> W	134.25±0.01	134	10.36±0.20	8.9±0.6	0
<sup>187</sup> W	479.53±0.01	479.4	26.6±0.4	30±1.8	0
<sup>187</sup> W	551.55±0.01	551.3	6.14±0.10	7.2±1	0
<sup>187</sup> W	618.37±0.01	618.2	7.57±0.12	7.8±1.1	0
<sup>187</sup> W	685.81±0.01	685.7	33.2±0.5	33.2±2	0
<sup>187</sup> W	772.87±0.02	772.6	5.02±0.08	5.8±1	0
<sup>116</sup> In	138.29±0.02	138.1	3.70±0.09	2.3±0.2	4.4±1.0
<sup>116</sup> In	355.40±0.02	355.4	0.730±0.011	1±0.3	0
<sup>116</sup> In	416.90±0.02	416.8	27.2±0.4	27.1±1.3	0
<sup>116</sup> In	818.68±0.02	818.6	12.13±0.14	11.8±0.9	0
<sup>116</sup> In	1097.28±0.02	1097.4	58.5±0.8	59.1±2.8	0
<sup>116</sup> In	1293.56±0.02	1293.7	84.8±1.2	84.7±3.8	0
<sup>116</sup> In	1507.59±0.02	1507.8	9.92±0.13	12±1	0
<sup>116</sup> In	2112.29±0.02	2112.7	15.09±0.22	15.4±1.3	0
<sup>52</sup> V	1434.06±0.01	1434.3	100.0±1.4	N/A	0
<sup>56</sup> Mn	846.76	846.5	98.85	106.5±8.2	12.6±0.6
<sup>56</sup> Mn	1810.73	1810.4	26.9±0.4	24.2±3.7	0
<sup>56</sup> Mn	2113.09	2112.9	14.2±0.3	13.8±3.1	0

**Table 7:** Spectra of produced isotope. The literature values are from Ref. (1). For the literature values if an uncertainty is not given, this means that the uncertainty is too small to be seen given the number of significant figures quoted. The uncertainties in the measured energy are discussed in the text.

In the table, the measured energy was calculated by finding the average energy of counts in the peak. Since the channel width was about 0.548 keV, the error in the measured energies should be



about half this value. Unfortunately due to a lack of time, a more rigorous calculation of the measured energy and calculation of the associated uncertainty could not be performed. The largest difference between the literature energy and the measured energy is 0.5 keV and the average absolute difference is 0.17 keV. Hence we can see that our measured energies agree quite well with the literature peaks energies.

Most peaks which had least a few percent chance of a count per decay were visible. The exceptions to this were the low energy peaks of  $^{187}\text{W}$  and  $^{198}\text{Au}$ , which were too small to be seen against the  $^{212}\text{Pb}/^{214}\text{Pb}$  x-rays.

To calculate the intensity of each peak, we first used the literature gamma ray intensities to calculate the total number of decays, combining the values from each peak in the standard way to find the best value. The measured intensity was then calculated as the ratio of the counts in the peak to the total number of decays multiplied by the energy efficiency. As  $^{52}\text{V}$  has only one characteristic peak, it was not possible to calculate the intensity for this peak.

Our measured intensities are in very good agreement with the literature values. Calculating the standard deviations that our measured intensities are from their literature values, we find that the average deviation is  $0.04\sigma$  and the standard deviation of the deviations is  $1.1\sigma$ . This is very close to the 0 average deviation and  $1\sigma$  standard deviation we would expect for a perfect error analysis with arbitrarily many samples. The only significant difference between the measured intensity and the literature intensity was for the 138 keV  $^{116}\text{In}$  peak. Our measured intensity is only about  $62\pm 7\%$  of the literature value. One possible explanation of this discrepancy is gamma ray self-shielding. For a 2mm thick sample of indium, the self-shielding effect at 138 keV would result in about a 40% gamma ray loss, but for the other, higher energy peaks, self-shielding effects would only cause between a 3% and 8% loss. Considering the size of the uncertainties for the higher energy peaks, the self-shielding would not be noticeable except for the 138 keV peak. As the other samples (with the exception of monoenergetic vanadium) were much thinner than the indium sample, this explains why self-shielding is only relevant for indium.

## 3.4 Half-Life Calculations

### Methodology

To calculate the half-life of our produced isotopes, we need to calculate some quantity that is proportional to the total number of decays for each time interval, and then perform a Bayesian fit to the exponential decay  $Ae^{-\lambda t}$ . Marginalising over the constant  $A$  (ie, assuming a flat prior over  $A$  and then integrating over this variable) allows us to calculate  $\lambda$  and its uncertainty

Initially, the total number of counts in the spectrum was used as the decaying quantity. There were two issues with this method. Firstly, the number of background counts was often much greater than the number of counts from our isotopes. For instance, in the case of  $^{187}\text{W}$ , the background contributed over 90% of the counts initially, and as the isotope decayed this increased to over 97%. Because the background was so large, this resulted in large uncertainties. The second problem was that, though the background could be calculated from the background spectrum, and was found to be  $1.801 \pm 0.013$  counts per second, it seems that the background by considerably more between different samples. Changing the background number of counts by even a few percent results in significant changes to the half-life calculated, and so without very accurate knowledge of the background, it was not possible to accurately calculate the half-life.

Instead, I decided to only use the counts in the vicinity of the characteristic peaks identified in *Table 2*. I summed over the channels that were within 2.5 keV of the centre of each peaks. I then performed a background subtraction using the same method that I used in the previous section to identify peaks, by first removing outlying channels with  $\sigma > 2$ , and then averaging over the remaining channels to calculate the background. Code for the entire procedure can be found in *Appendix 1*.

### Results

The measured half-lives are given in *Table 8*. These are compared to the half-lives from Ref. (1). For the cases where I have multiple spectra for the same isotope, I have listed the separately measured half-lives and then combined them in the standard way to get the best possible half-life value. In *Figure 6* and *7*, lifetime curves are shown for one of the indium samples and the tungsten sample. The best lifetime and  $A$  value is plotted for the data set.

Spectrum	Measured half-life (s)	Literature Half-Life (s)	Spectrum	Measured half-life (s)	Literature Half-Life (s)
$^{198}\text{Au}$	$242244 \pm 6652$	$232820 \pm 30$	$^{187}\text{W}$ (a)	$66923 \pm 3625$	$86400 \pm 15$
$^{116}\text{In}$ (0.5h)	$3375 \pm 526$		$^{187}\text{W}$ (b)	$80049 \pm 7351$	$86400 \pm 15$
$^{116}\text{In}$ (1h)	$2232 \pm 438$		$^{56}\text{Mn}$	$9801 \pm 1775$	$9284.0 \pm 0.3$
$^{116}\text{In}$ (1.5h)	$3929 \pm 706$		$^{52}\text{V}$ (Tues)	Insufficient Points	
$^{116}\text{In}$ (2h)	$4211 \pm 670$		$^{52}\text{V}$ (Thurs)	$213 \pm 79$	
$^{116}\text{In}$ (2.5h)	$3451 \pm 588$		$^{52}\text{V}$ (Fri)	$272 \pm 75$	
$^{116}\text{In}$ (3h)	$3519 \pm 625$		Combined	$244 \pm 54$	$224.6 \pm 0.3$
Combined	$3246 \pm 232$	$3257 \pm 10$			

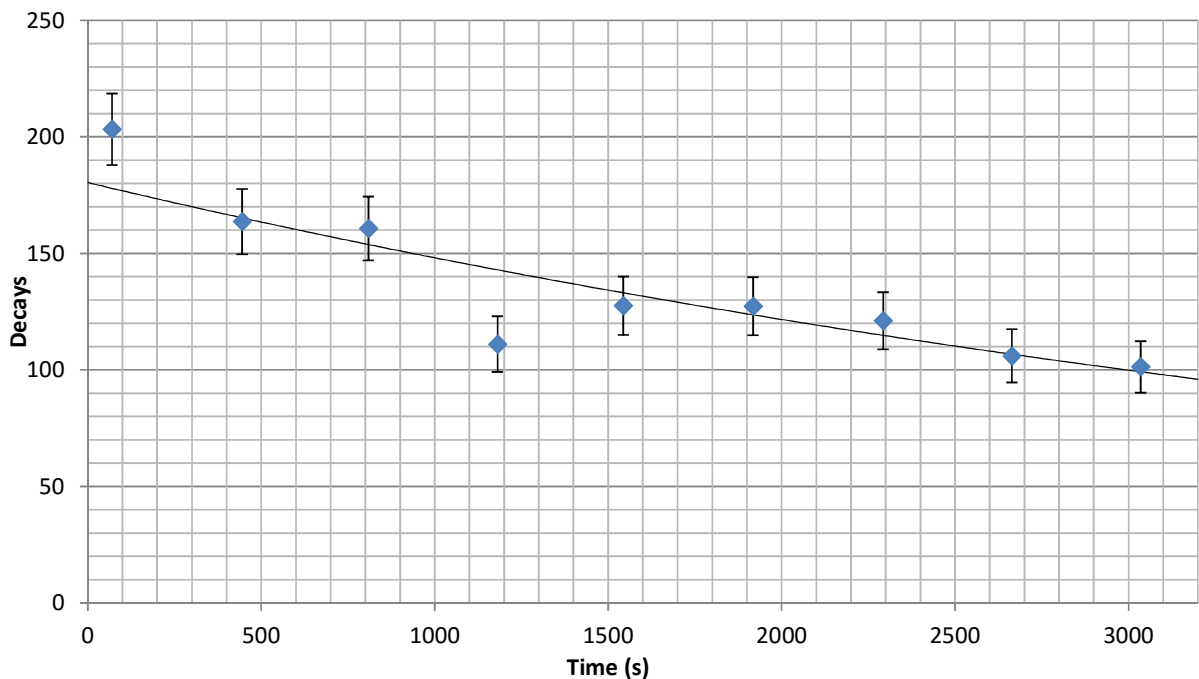
**Table 8:** Measured half-lives.

Note that in *Table 3*, the Tuesday  $^{52}\text{V}$  spectrum was unable to be used as the count rate in the peak was too low to give a meaningful answer; the rate was zero for all but the first two time intervals. Also note that the half-life of  $^{187}\text{W}$  is calculated twice. For the  $^{187}\text{W}$  (a) row, all the peaks were used, but for the  $^{187}\text{W}$  (b) peak, only the 479.53 keV peak and 685.81 keV peak were used.

Our measured half-lives agree with the literature values. Other than the  $^{198}\text{Au}$  and  $^{187}\text{W}$  (a), the measured half-lives were within  $1\sigma$  of their literature values, and even the  $^{198}\text{Au}$  half-life was only out by  $1.4\sigma$ . For  $^{187}\text{W}$  (a) however, the measured half-life was over  $5\sigma$  larger than the literature value. Since two of the most intense  $^{187}\text{W}$  peaks lie in the low energy part of the spectrum where there are numerous background peaks, I thought the error may have been caused by interference from nearby peaks. For this reason, I recalculated the half-life using only the 479.53 keV peak and 685.81 keV, which are the two most intense peaks above 200 keV. This half-life agrees quite well with the literature half-life.

The relative size of the uncertainties varies considerably between the isotopes. The smallest uncertainty was for  $^{198}\text{Au}$ , which had a relative uncertainty of only 2.7%, whereas the uncertainty in the  $^{52}\text{V}$  half-life was 22%. This is due to the small number of  $^{52}\text{V}$  decays observed compared to  $^{198}\text{Au}$ . To get more precise measurements of the isotope half-lives, we need to increase the number of decays, either with more trials, more massive samples, or a stronger neutron source. Since the uncertainty in a Poissonian distribution is proportional to  $\sqrt{n}$ , to increase the precision by a factor of  $A$  we would need roughly  $A^2$  counts. Hence to improve the precision by a significant factor, we need a stronger neutron source, as using kilogram samples or performing hundreds of trials is quite difficult.

**Figure 6:** Lifetime curve for the 3 hour indium sample. The curve plotted has  $\frac{1}{\lambda} = 3519$  s and  $\ln(A) = 5.20$ .



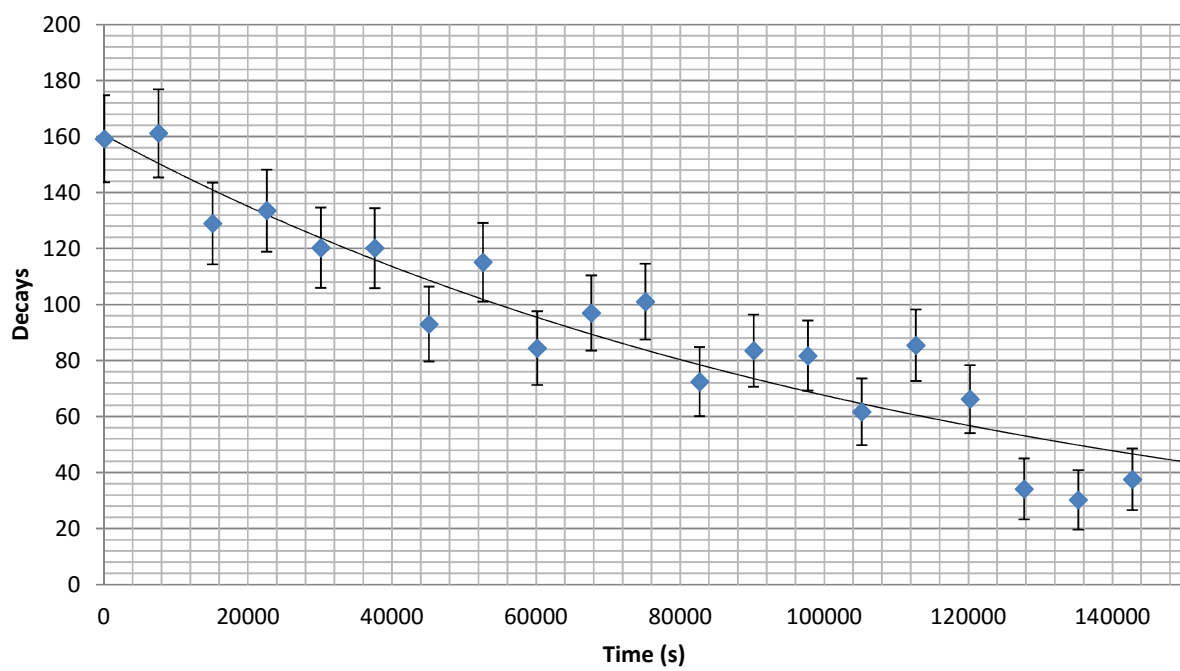


**Figure 7:** Lifetime curve for the tungsten sample. The plotted curve has  $\frac{1}{\lambda} = 80050$  s and  $\ln(A) = 5.08$ .

### 3.5 Isotope Yields and Neutron Flux

To calculate the neutron flux, we need to calculate the number of activated nuclei initially. As discussed in the introduction, the fraction of decays that our measurements captured is

$$(1 - e^{-\lambda h}) \sum_i e^{-\lambda t_i}$$

where the  $t_i$ 's are the time at which the individual measurements began, and  $h$  is the length of each measurement. So if we sum over all the spectra in each trial, then by finding the number of counts,  $C$ , in some characteristic peak, we can calculate the total initial number of radioactive nuclei as

$$N_0 = \frac{C}{\varepsilon I (1 - e^{-\lambda h}) \sum_i e^{-\lambda t_i}}$$

where  $\varepsilon$  is the energy efficiency at the peak energy and  $I$  is the peak intensity.

To calculate  $C$  for a given peak, I used the same method as for the half-life calculations. I summed over all the counts within 2.5 keV of the peak, and then performed a background subtraction using channels where  $\sigma < 2$ .

Once we have calculated the total number of nuclei from each of the characteristic peaks, we can then combine these to get the best possible value for this quantity.

From this quantity, we can then calculate the neutron flux using the formula

$$\phi = \frac{\lambda N_0}{\sigma N_A (1 - e^{-\lambda t})}$$

as discussed in the introduction. Here we take the literature value of the decay constant  $\lambda$ . We use the cross section  $\sigma$  and total activatable nuclei  $N_A$  calculated in the introduction. The results are shown in *Table 9*.

Sample	Initial Number of Activated Nuclei	Neutron Flux (cm <sup>-2</sup> s <sup>-1</sup> )	Sample	Initial Number of Activated Nuclei	Neutron Flux (cm <sup>-2</sup> s <sup>-1</sup> )
Indium (0.5h)	220900±7100	12.37±0.57	Vanadium (Tuesday)	2680±950	34.09±17.45
Indium (1h)	174800±7600	11.80±0.74	Manganese	140200±6700	42.94±2.95
Indium (1.5h)	143500±5500	13.70±0.75	Tungsten	407300±14900	158.4±8.4
Indium (2h)	176100±6200	8.12±0.41	Gold	5795600±181300	45.24±2.04
Indium (2.5h)	189700±6400	16.95±0.82			
Indium (3h)	184300±6400	13.38±0.66			

**Table 9:** Number of nuclei produced and implied neutron flux

In *Table 9*, the uncertainty in the neutron flux is from the uncertainty in the number of active nuclei present. It does not include the uncertainty in the placement of the sample relative to the neutron source. The samples were placed 5cm from the centre of the source, but the uncertainty in this placement was about 0.5cm. Considering that the neutron flux should follow a  $1/r^2$  law, this suggests that the uncertainty in the flux from geometric considerations should be about 20%.

With this in mind, the indium flux measurements can be seen to be consistent with each other. The vanadium, manganese, and gold measurements are similar consistent. Combining the indium flux values gives us a best value of  $11.45 \pm 0.99 \text{ cm}^{-2}\text{s}^{-1}$ , whereas combining the vanadium, manganese, and gold values gives us a best value of  $43.00 \pm 6.13 \text{ cm}^{-2}\text{s}^{-1}$ . These values clearly do not agree with each other, and nor do they agree with the flux calculated from the tungsten sample of  $158.36 \pm 32.76 \text{ cm}^{-2}\text{s}^{-1}$ .

Our neutron source emitted around 59000 neutrons per second, and so assuming a spherical distribution of neutrons, the neutron flux at 5cm should be  $187.8 \text{ cm}^{-2}\text{s}^{-1}$ . This value is considerably higher than any of the fluxes we have calculated. We now have two problems; explaining why our calculated fluxes don't match the predicted flux, and explaining why our calculated fluxes are not consistent with each other.

One possibility is that the neutrons have not been sufficiently thermalised at 5cm. This would mean that the thermal cross sections we've used are not the correct cross sections. Since the dependence of the neutron cross section on energy can be quite complicated in general, it is difficult to predict how this would in practise effect the calculated flux.

A second issue is that our calculations don't take into consideration neutron self-shielding. Since the nuclei in our sample are absorbing and scattering neutron radiation, the neutron flux will decrease through the sample. This effect would result in an underestimation of the neutron flux.

With these considerations, it seems the simplest ways to improve our calculation of neutron flux would be to place the samples further from the source, as this would increase the thermalisation of the neutrons and so allow us to use the thermal neutron cross section. Placing the sample further away would also decrease the uncertainty in the placement of the source, as the relative uncertainty of say  $10 \pm 0.5\text{cm}$  is half that of  $5 \pm 0.5\text{cm}$ . For a greater reduction in this source of uncertainty, a more precise method of placing the samples could be developed, for instance by using fixed markers to place the samples next to.

### 3.6 Unknown Sample Analysis

We will now attempt to calculate the composition of the unknown sample. By identifying the peaks that I found in the unknown spectrum, I found evidence of  $^{116}\text{In}$ ,  $^{187}\text{W}$ , and  $^{198}\text{Au}$ . I then used the same method as the previous section to calculate the initial number of radioactive nuclei immediately after irradiation ended. Rearranging the formula

$$\phi = \frac{\lambda N_0}{\sigma N_A (1 - e^{-\lambda t})}$$

used in the previous section, we can find the total number of activatable nuclei as

$$N_A = \frac{\lambda N_0}{\sigma \phi (1 - e^{-\lambda t})}.$$

For the value of  $\phi$ , we can use the neutron fluxes found for each of the isotopes in the previous question. Once  $N_A$  is known, the mass of the element can be calculated from the atomic mass and the isotopic abundance of the isotope that was activated. The results are given in *Table 10*.

Element	Calculated Mass (g)	Actual Mass (g)
Indium	0.426±0.176	0.199
Tungsten	1.459±0.529	1.968
Gold	1.172±0.408	1.02

**Table 10:** Composition of the unknown sample. The calculated mass column gives the mass of each element as found through the neutron activation analysis, and the actual mass column gives the mass found by measuring the constituent elements of the unknown sample.

As we can see in *Table 10*, the neutron activation analysis provided a reasonable value for the masses of indium, tungsten and gold. Unfortunately, the uncertainties in the masses of indium, tungsten, and gold are massive. Most of this uncertainty originated from the uncertainty in the placement of the unknown sample, along with the uncertainty in the neutron flux from the placement of the samples used to calculate the neutron flux. In order to accurately calculate the composition of the unknown sample; we need to be far better at controlling these uncertainties.

While we didn't find any evidence of vanadium or manganese, this doesn't necessarily mean that they aren't present, but simply that the amount present was too small to be seen over the background. For a peak to be  $3\sigma$  above the background half the time, we would require that

$$C \geq 3\sqrt{tN_B}$$

where  $C$  is the number of counts in the photopeak, and  $N_B$  is the background count rate, and  $t$  is the time measured over. Now using the fact that

$$C = \epsilon I N_A (1 - e^{-\lambda t})$$

where  $N_A$  is the number of active nuclei at the start of the measurement,  $\varepsilon$  is the energy efficiency of the peak, and  $I$  is the peak intensity, we find that

$$N_A \geq \frac{\sqrt{tN_B}}{\varepsilon I(1 - e^{-\lambda t})}.$$

If less than  $N_0$  of the active nuclei are present, then there is a greater than 50% chance that the nuclei will not be detected. The formula

$$N_A = \frac{\lambda N_0}{\sigma \phi(1 - e^{-\lambda t})}.$$

allows us to find the minimum number of activatable nuclei in the sample, and using the isotopic abundance and atomic mass we can then convert this into a minimum detectable mass. We can use this to calculate the maximum amount of vanadium and manganese that could be in the unknown sample. The best peak to detect manganese is the 846 keV peak, as this peak has the highest intensity. The background at this location was found to be 12 counts per hour. We can minimise  $N_A$  by taking the first nine measurements, corresponding to  $t = 16200$  s, and hence find that if there was 0.055g of manganese, this would only be detected half of the time. For vanadium, the only peak we can use is the 1434 keV peak. At this location there is a background of 8 counts an hour, and  $N_A$  is minimised if we only take the first measurement, corresponding to  $t = 1600$  s. We find that 1.66g of vanadium would be detected about half the time. We can hence see that while our neutron activation analysis is quite sensitive to the manganese, it is terrible at detecting vanadium and it is quite possible that vanadium is a major component of the unknown sample.



## 4. Conclusion

We studied the neutron activation of indium, vanadium, manganese, tungsten and gold by using a high purity germanium detector to measure the spectra of the produced isotopes. This allowed us to find the characteristic gamma ray peaks of  $^{116}\text{In}$ ,  $^{52}\text{V}$ ,  $^{56}\text{Mn}$ ,  $^{187}\text{W}$ , and  $^{198}\text{Au}$ . The peak energies and intensities of these peaks were measured, and the half-lives of the isotopes evaluated. We found that these values were in agreement with the values found in the NNDC. To more accurately calculate these quantities, we would simply need to monitor more decays, and so the most pragmatic way to greatly improve the accuracy of our measurements would be to use a stronger neutron source. Smaller improvements could be gained through larger sample masses and repeated measurements.

We attempted to calculate the flux of our neutron source using thermal capture cross sections, however, this proved unsuccessful as our samples were too close to the source to give adequate neutron thermalisation. To get more accurate flux values, a larger distance from the source should be used, say 10cm from the source rather than the 5cm we used. The ability of neutron activation as an analytic technique was tested, and we were able to crudely determine the composition of an unknown sample. The biggest source of uncertainty in this analysis was from the uncertainty in the irradiation geometry. While the activation analysis was able to put significant upper bounds on the quantity of manganese that could be present in the unknown sample, it was not very sensitive to vanadium and may not have detected over 1.66g of vanadium.

## 5. Bibliography

---

1. **National Nuclear Data Center.** Chart of Nuclides. *National Nuclear Data Center*. [Online] [Cited: 28 04 2015.] <http://www.nndc.bnl.gov/chart/>.
2. **Barbalace, Kenneth.** Periodic Table of Elements - Sorted by Cross Section (Thermal Neutron Capture). *Environmental Chemisry*. [Online] 22 2 2007. [Cited: 5 May 2015.] <http://environmentalchemistry.com/yogi/periodic/crosssection.html>.
3. **National Institute of Standards and Technology.** Atomic Weights and Isotopic Compositions for All Elements. *Nation Institute of Standards and Technology Website*. [Online] 30 01 2015. [Cited: 06 05 2015.] [http://physics.nist.gov/cgi-bin/Compositions/stand\\_alone.pl?ele=&ascii=html&isotype=some](http://physics.nist.gov/cgi-bin/Compositions/stand_alone.pl?ele=&ascii=html&isotype=some).
4. **ORTEC.** Experiment 17: Neutron Activation Analysis. *Ortec Online*. [Online] [Cited: 04 05 2015.] [www.ortec-online.com](http://www.ortec-online.com).
5. **Debertin, K and Helmer, R.G.** *Gamma and X-Ray Spectrometry with Semiconductor Detectors*. Amsterdam : Elsevier Science Publishers, 1988.
6. **Firestone, R.B. and Ekström, L.P.** WWW Table of Radioactive Isotopes. *LBNL Isotopes Project*. [Online] January 2004. [Cited: 28 April 2015.] <http://ie.lbl.gov/toi/>.
7. **Gilmore, Gordon.** Appendix D:Gamma-Ray Energies in the Detector Background and the Environment. *Practical Gamma-Ray Spectroscopy*. s.l. : Wiley, 2011.

## Appendix 1: Python Scripts

While I wrote numerous scripts to analyse the lab data, for the sake of brevity I've only included the two most interesting and important scripts. The first is the peak finding script, and the second is the half-life finding script. They have been written in *Python 3.4*.

### A1.1 Peak finder script

```
import math

peaks = #List of literature characteristic gammas with format (energy,"source",additional_info)
back_data = []

found = []
identified = []

data = #list of form [(energy of channel, counts in channel)]

#Finds channels which are probably part of the background
chan_max = 50
chan_min = 10
for i in range(18,3969-chan_max):
    count = math.ceil(data[i][1])
    background = 0
    for j in range(chan_min,chan_max):
        background += data[i-j][1]+data[i+j][1]

    if background == 0:
        break

    background = background/(2*(chan_max-chan_min))
    sigma = (count-background)/math.sqrt(count+background)

    if sigma>2:
        back_data[i] = False

#finds peaks in the spectra, and calculates their energy
#and total counts in the peak, along with the background
in_peak = False
min_energy = 0
max_energy = 0
total_counts = 0
total_background = 0
mean_energy = 0

for i in range(18,3969-chan_max):
    count = math.ceil(data[i][1])
    background = 0
    channels = 0
    for j in range(1,chan_max):
        if back_data[i-j] and back_data[i+j]:
            background += data[i-j][1]+data[i+j][1]
            channels += 1
```

```

if background == 0:
    break

background = background/(2*channels)
sigma = (count-background)/math.sqrt(count+background)

if sigma>1:
    if in_peak == False:
        min_energy = data[i][0]
    in_peak = True
    total_counts += data[i][1]
    total_background += background
    mean_energy += (data[i][0]-0.548/2)*(data[i][1]-background)

elif in_peak:
    max_energy = data[i-1][0]
    in_peak = False
    sigma = (total_counts-total_background)/math.sqrt(total_counts+total_background)
    if sigma>2.5:
        peak_number += 1
        mean_energy = mean_energy/(total_counts-total_background)
        found +=
[(min_energy,max_energy,sigma,total_counts,total_background,mean_energy)]

#this identifies the peaks with peaks in the peak list
id_peaks = []
for j in peaks:
    if min_energy<j[0] and max_energy>j[0]:
        id_peaks += [j]
identified += [id_peaks]

min_energy = 0
max_energy = 0
mean_energy = 0
total_counts = 0
total_background = 0

```

## A1.2 Half-Life Calculator

```
import math

def channel(E):
    return math.floor((E-calibration_0)/calibration_grad+.5)

times = #list of start times for the measurements
peaks = #list of characteristic gamma peaks

width = 4

time_counts = []
for file_num in range(1,number_files):
    data = #list of [(channel energy, peak counts)] for the specific data file

    #This finds the channels which are in the background
    chan_max = 50
    chan_min = 10
    back_data = [True for i in range(0,4000)]
    for i in range(18,3969-chan_max):
        count = math.ceil(data[i][1])
        background = 0
        for j in range(chan_min,chan_max):
            background += data[i-j][1]+data[i+j][1]

        if background == 0:
            break

        background = background/(2*(chan_max-chan_min))
        sigma = (count-background)/math.sqrt(count+background)
        if sigma>2:
            back_data[i] = False

    #this sums over the counts in the characteristic peaks
    total_count = 0
    total_var = 0
    for j in range(len(peaks)):
        C_E = channel(peaks[j])
        background = 0
        channel_num = 0
        for i in range(chan_min,chan_max):
            if back_data[C_E+i] and back_data[C_E-i]:
                background += data[C_E+i][1]+data[C_E-i][1]
                channel_num += 2

        background = background/channel_num*(2*width+1)
        uncrt_back = math.sqrt(background)/channel_num*(2*width+1)

        counts = data[C_E][1]
        for i in range(1,width+1):
            counts += data[C_E+i][1]+data[C_E-i][1]

        total_var += counts+uncrt_back**2
```

```

    total_count += counts - background
    time_counts += [(times[file_num-1],total_count,1/(2*total_var))]

def Chi2(l,c):
    output = 0
    for i in time_counts:
        rate = math.exp(c-i[0]/l)
        output += (rate-i[1])**2*i[2]
    return math.exp(-output)

C_min = #Boundary for integral
C_max = #Boundary for integral
C_steps = #Number of intervals
C_h = (C_max-C_min)/C_steps

L_min = #Boundary for integral
L_max = #Boundary for integral
L_steps = #Number of intervals
L_h = (L_max-L_min)/L_steps

#integrates probability distribtuion
norm = 0
av_l = 0
square_l = 0
av_c = 0
square_c = 0
for i in range(0,C_steps):
    c = C_min + i*C_h
    for j in range(0,L_steps):
        l = L_min+j*L_h
        P = Chi2(l,c)
        norm += P
        av_l += l*P
        square_l += l**2*P
        av_c += P*c
        square_c += P*c**2

av_l = av_l/norm
square_l = square_l/norm
av_c = av_c/norm
square_c = square_c/norm

print("Half-Life",av_l*math.log(2),math.sqrt(square_l-av_l**2)*math.log(2))

```

## Appendix 2: Characteristic Peak Identification

### A2.1 Background Peaks

In these tables, the nuclide column contains the specific nuclide responsible for the gamma ray. The relative intensity of the peak is defined as the intensity of the peak multiplied by the energy efficiency at the peak energy; this quantity gives us the probability that a decay will result in a count in the photopeak. There is implicitly an uncertainty in this value from the uncertainty in the energy efficiency, of 6.15% for peaks with energy less than 120keV and 3.12% otherwise. This uncertainty has been suppressed in the table for brevity. The gold, tungsten, and background counts per hour column give the predicted number of decays per hour, calculated by dividing the number of counts in the peak per hour by the relative intensity of the peak. The "other poss." column has a no if no other possible sources of the gamma were found, and yes otherwise.

#### <sup>238</sup>U Series

Energy (keV)	Nuclide	Relative Intensity (%)	Au Counts (per hour) (x100)	Other Poss.	W Counts (per hour)	Other Poss.	Background Counts (per hour) (x100)	Other Poss.
46.54	210Pb	0.08987	35.0 ± 11.4	No	47.0 ± 12.1	No		
53.23	214Pb	0.02988	96.9 ± 28.7	Yes				
63.28	234Th	0.17809	40.9 ± 6.2	No	24.2 ± 5.3	No		
92.58	234Th	0.28883	33.8 ± 4.0	Yes	50.6 ± 5.0	Yes		
186.21	226Ra	0.12109	51.6 ± 8.8	No	54.0 ± 9.0	No		
242	214Pb	0.19228	383.1 ± 11.2	Yes	395.5 ± 10.8	Yes	82.6 ± 22.4	Yes
295.22	214Pb	0.40405	48.9 ± 2.6	No	46.6 ± 2.9	No	50.2 ± 9.6	No
351.93	214Pb	0.65633	53.5 ± 1.7	No	46.0 ± 1.9	Yes	57.7 ± 7.1	Yes
609.31	214Bi	0.49398	42.9 ± 1.6	No	40.7 ± 2.0	No	35.9 ± 6.2	No
768.36	214Bi	0.04246	56.0 ± 11.1	No	45.7 ± 11.3	No		
934.06	214Bi	0.02227	49.1 ± 14.6	No				
1120.29	214Bi	0.08998	48.4 ± 4.7	No	50.4 ± 6.0	No		
1238.11	214Bi	0.03194	63.3 ± 9.6	Yes	71.5 ± 12.6	Yes		
1377.67	214Bi	0.01962	43.4 ± 11.5	No	56.4 ± 16.2	No		
1729.6	214Bi	0.01129	49.4 ± 16.1	No				
1764.49	214Bi	0.05951	64.9 ± 5.6	No	62.0 ± 6.9	No		

**Table A1:** Peaks of <sup>238</sup>U found in the background.

All of the peaks with a relative intensity above 0.016 were detected in the Gold spectrum, and the predicted number of decays per hour is very uniform amongst the peaks where no other decay was found to be possible. If we combined these count rates in the standard way then we find that the rate of <sup>238</sup>U series decays per hour is 4653±80.

## <sup>232</sup>Th Series

Energy (keV)	Nuclide	Relative Intensity (%)	Au Counts (per hour) (x100)	Other Poss.	W Counts (per hour) (x100)	Other Poss.	Background Counts (per hour) (x100)	Other Poss.
72.81	208Ti	1.21113			13.5 ± 1.2	Yes		
74.97	208Ti	2.07786	64.7 ± 1.3	Yes	45.1 ± 1.2	Yes	16.5 ± 2.6	Yes
87.3	208Ti	0.19693	73.0 ± 6.8	Yes	82.9 ± 7.4	Yes		
129.06	228Ac	0.11739	39.5 ± 9.5	No	25.4 ± 8.1	No		
209.26	228Ac	0.1184	35.9 ± 8.5	No	31.8 ± 8.4	No	89.3 ± 34.4	No
238.63	212Pb	1.16916	63.0 ± 1.8	Yes	65.0 ± 1.8	Yes	43.3 ± 4.8	No
240.89	224Ra	0.10948	672.8 ± 19.7	Yes	694.5 ± 19.0	Yes	145.1 ± 39.4	Yes
270.24	228Ac	0.08229	25.4 ± 8.0	No	29.4 ± 10.0	No		
277.37	208Tl	0.05497			39.8 ± 12.3	No		
300.09	212Pb	0.06837			50.1 ± 11.6	Yes		
328	228Ac	0.05821			26.2 ± 10.3	No		
338.32	228Ac	0.21583	38.3 ± 3.2	Yes	35.1 ± 4.2	Yes		
409.46	228Ac	0.03059	22954.3 ± 115.2	Yes				
463	228Ac	0.06227	32.2 ± 7.6	Yes				
510.7	208Tl	0.08098	650.0 ± 15.8	Yes	643.6 ± 19.7	Yes	613.0 ± 68.5	Yes
583.19	208Tl	0.34663	34.8 ± 1.9	No	39.3 ± 2.4	Yes		
727.33	212Bi	0.0617	27.7 ± 5.9	No	37.3 ± 9.1	Yes		
794.95	228Ac	0.03571	31.6 ± 9.1	No	34.0 ± 11.2	No		
860.56	208Tl	0.03487	27.0 ± 9.0	No			49.1 ± 12.2	No
911.2	228Ac	0.19005	39.7 ± 2.7	No	40.5 ± 3.3	No		
964.77	228Ac	0.03479	54.5 ± 11.5	No	34.2 ± 4.3	No	43.3 ± 16.8	No
968.97	228Ac	0.10969	46.5 ± 4.6	No				
1588.2	228Ac	0.01388	55.7 ± 16.4	No				

**Table A2:** Peaks of <sup>232</sup>Th found in the background

While the <sup>232</sup>Th peaks I did not detect had for the most part relative intensities below 0.01, the 84.94 <sup>208</sup>Ti peak was not visible on any of the spectra, even though its relative intensity was 0.53036. This is probably due to the presence of more intense peaks around this region from other sources. Again combining Bayesian the peaks where no other gamma source was found, the <sup>232</sup>Th series decay rate was calculated to be 3688±110 counts per hour.

## Other High Energy Peaks

In the below table, if the relative intensity column is empty, this means that the intensity of the decay was not given in the table, usually because the decay is caused by secondary excitation of the detector or shielding products.



Energy (keV)	Nuclide	Relative Intensity (%)	Au Counts (per hour) (x100)	Other Poss.	W Counts (per hour) (x100)	Other Poss.	Background Counts (per hour) (x100)	Other Poss.
53.44	<sup>73</sup> mGe	0.29356	9.9 ± 2.9	Yes				
68.75	<sup>73</sup> Ge		Detected	Yes				
74.82	<sup>212</sup> Pb, <sup>214</sup> Pb X-ray	1.24349	108.1 ± 2.2	Yes	75.4 ± 2.0	Yes	27.5 ± 4.3	Yes
77.11	<sup>212</sup> Pb, <sup>214</sup> Pb X-ray	2.131	63.1 ± 1.3	Yes	44.0 ± 1.1	Yes	24.7 ± 2.8	No
87.35	<sup>212</sup> Pb, <sup>214</sup> Pb X-ray	0.5391	26.7 ± 2.5	Yes	30.3 ± 2.7	Yes		
89.78	<sup>212</sup> Pb, <sup>214</sup> Pb X-ray	0.20078			36.4 ± 6.0	Yes		
139.68	<sup>75</sup> mGe	1.75286	2.5 ± 0.6	No	2.9 ± 0.8	No		
198.39	<sup>71</sup> mGe		Detected	No	Detected	No		
511	Annihilation		Detected	No	Detected	Yes	Detected	Yes
846.77	<sup>56</sup> Co	0.79014	16.0 ± 0.8	Yes	13.8 ± 0.9	Yes	16.0 ± 3.3	Yes
846.77	<sup>56</sup> Fe		Detected	Yes	Detected	Yes	Detected	Yes
1238.29	<sup>56</sup> Co	0.36422	5.5 ± 0.8	Yes	6.3 ± 1.1	No		
1460.82	<sup>40</sup> K	0.04981	104.9 ± 8.0	No	111.8 ± 10.0	No	74.4 ± 28.3	No

**Table A3:** Other high energy peaks found in the background.

This table includes all the other identified peaks with energy above 50keV. In the low energies, <sup>212</sup>Pb and <sup>214</sup>Pb X-rays can clearly be seen; these radioactive isotopes occur in the <sup>234</sup>Th and <sup>238</sup>U decay series respectively. The <sup>40</sup>K peak is quite clear, and combining the three different values for the amount of decay gives us a decay rate of 10599±610 counts per hour. <sup>56</sup>Co could plausibly be present, but since both its peaks lie near other peaks, it is difficult to verify whether it is actually present. The annihilation peak is caused by the annihilation of positrons with electrons, and there are contributions to this curve from all of the nuclides which undergo beta decay. Hence this peak is not particularly useful for determining constituents of the background.

The other peaks listed are caused by excitation of either the germanium in the detector, or for the 846.77keV peak, possible excitation of the iron shield.

## Quantity of Primordial Elements

The activity of a source is related to the number of nuclei by

$$A_0 = \lambda N_0 = \frac{\ln(2)}{h} N_0$$

for  $A_0$ , decay constant  $\lambda$ , half-life  $h$  and number of nuclei  $N_0$ . Hence to find the mass of an element present given an activity  $A_0$ , we get the formula

$$m = \frac{A_0 h M}{\ln(2) I N_A}$$

where  $m$  is the mass,  $I$  the isotopic abundance of the radioisotope,  $M$  the molar mass of the element, and  $N_A$  is Avogadro's number. We can now calculate the quantities of uranium, thorium,

and potassium present around the detector, assuming that the quantities are located on top of the detector. In *Table A4*, the quantity of these elements are found, with the values for the constants found from the NNDC database.

Element	Radioisotope	Activity (per hour)	Isotopic Abundance (%)	Half-Life ( $\times 10^9$ years)	Atomic Mass of Element (u)	Mass Present (mg)
Uranium	$^{238}\text{U}$	4653 $\pm$ 80	99.27	4.47	238.029	0.105 $\pm$ 0.002
Thorium	$^{232}\text{Th}$	3688 $\pm$ 110	100	14	232.038	0.251 $\pm$ 0.007
Potassium	$^{40}\text{K}$	10599 $\pm$ 610	1.17 $\pm$ 0.01	1.25	39.098	0.929 $\pm$ 0.053

**Table A4:** Calculation of the quantities of primordial elements.

## A2.2 Sample Peaks

The following tables document all the peaks for these isotopes with intensity greater than 0.1%. In the tables, the relative intensity is again defined as the product of the peak intensity with photopeak efficiency at that energy; again the uncertainty due to energy efficiency has been suppressed for brevity. The calculated total decays column shows the total number of decays calculated using the relative intensity and the number of counts in the peak. The background peak column notes whether there are background peaks that could be alternative sources of the gamma rays. If there are none, then we would expect that the calculated total decay column should show a consistent number of total decays. This would provide confirmation that the peak intensities of the peaks are correct. For peaks where a background peak is present but not overwhelming, the count rate gives the background counts per hour expected at the peak; this value will be useful in future analysis. Note that the uncertainties in these values do not include the uncertainties from the energy efficiency uncertainties.

### $^{198}\text{Au}$ Spectrum

Energy	Measured Energy (keV)	Counts	Relative Intensities (%)	Calculated Total Decays ( $\times 100$ )	Background Peaks?	Count Rate (per hour)
68.89		N/ Bckgrnd	0.03273			
70.82		N/ Bckgrnd	0.05693			
79.82		N/ Bckgrnd	0.00764			
80.22		N/ Bckgrnd	0.01472			
82.473		Not Detected	0.00543			
411.8	411.99	42129 $\pm$ 211	1.51505	27807.2 $\pm$ 878.7	Yes	1.13 $\pm$ 0.3
675.88	676.3	161 $\pm$ 27	0.00791	20402.0 $\pm$ 3521.8	No	0
1087.6842		Not Detected	0.00099			

**Table A5:**  $^{198}\text{Au}$  spectrum observations

We can see that for the  $^{198}\text{Au}$  spectrum, the only useful peaks were the 411.8 and the 675.88 peaks. The other peaks were either not detected, or were overshadowed by background peaks. We can calculate the total number decays over the 60 hour spectrum as 27309 $\pm$ 853.

**<sup>187</sup>W**

Energy	Measured Energy (keV)	Counts	Relative Intensities (%)	Calculated Total Decays (x100)	Background Peaks?	Count Rate (per hour)
59.72			0.28531	9205.4 ± 649.4	Yes	
61.14			0.5058	5192.5 ± 366.3	Yes	
Combined	60.05	2626 ± 91	0.7911	2900.91±234.8	Yes	8.28±0.1
68.995		N/ Bckgrnd	0.06812			
69.31	69.41	394 ± 48	0.13155	2996.5 ± 409.2	No	0
71.95		N/ Bckgrnd	0.04795			
72		N/ Bckgrnd	0.58578			
134.25	134.33	1057 ± 61	0.48379	2183.9 ± 143.2	No	0
206.247		Not Detected	0.01583			
239.13		N/ Bckgrnd	0.00268			
246.2		Not Detected	0.00354			
479.53	479.74	1046 ± 42	0.36391	2875.5 ± 147.2	No	0
511.76		N/ Bckgrnd	0.01037			
551.55	551.62	218 ± 30	0.0734	2976.3 ± 424.8	No	0
582		N/ Bckgrnd	0.00443			
589.06		Not Detected	0.00168			
618.37	618.51	212 ± 28	0.08104	2619.4 ± 355.8	No	0
625.52		Not Detected	0.01391			
685.81	685.99	820 ± 36	0.32166	2548.4 ± 137.4	No	0
745.21		Not Detected	0.00329			
772.87	772.92	127 ± 20	0.04334	2939.8 ± 479.8	No	0
864.55		Not Detected	0.00317			
879.44		Not Detected	0.0013			

**Table A6:** <sup>187</sup>W spectrum observations

Using the peaks for which no background peak was present, we can calculate that there were 2606±72 decays. Note that the first two peaks could not be resolved and so their combined intensity has been used to calculate the total number decays. No other peaks were detected above the background.

**<sup>56</sup>Mn**

Energy	Measured Energy (keV)	Counts	Relative Intensities(%)	Calculated Total Decays (x100)	Background Peaks?	Count Rate (per hour)
846.76	846.84	591 ± 25	0.78154	756.7 ± 40.2	Yes	12.6±0.6
1810.73	1810.7	59 ± 8	0.10219	578.7 ± 84.3	No	0
2113.09	2113.16	29 ± 6	0.04648	627.3 ± 135.5	No	0

**Table A7:** <sup>56</sup>Mn spectrum observations

Using all three peaks, the total number of <sup>56</sup>Mn decays can be calculated to be 719±35.

**<sup>116</sup>In**

Energy	Measured Energy (keV)	Counts	Relative Intensities(%)	Calculated Total Decays (x100)	Background Peaks?	Count Rate (per hour)
138.29	138.42	405±32	0.16791	2414.2 ± 205.5	Yes	4.4±1
263.03		Not Detected	0.00308			
278.62		Not Detected	0.003			
303.73		Not Detected	0.00255			
355.4	355.68	67±17	0.01333	5049.4 ± 1310.2	No	0
416.9	417.06	1634±44	0.42589	3836.1 ± 157.6	No	0
463.21		Not Detected	0.01026			
655.17		Not Detected	0.00125			
688.93		Not Detected	0.0016			
705.97		Not Detected	0.00151			
779.12		Not Detected	0.00212			
818.68	818.94	371±23	0.09907	3743.0 ± 263.0	No	0
972.6		Not Detected	0.00343			
1097.28	1097.7	1398±39	0.36024	3880.2 ± 163.3	No	0
1293.56	1294.02	1713±42	0.44556	3844.4 ± 152.8	No	0
1507.59	1508.14	209±15	0.04497	4649.8 ± 371.8	No	0
1752.5		Not Detected	0.00925			
2112.29	2112.99	205±15	0.04941	4139.4 ± 327.7	No	0

**Table A8:** <sup>116</sup>In spectrum observations

The only detected peak in <sup>116</sup>In with possible background peak interference is the 138.29 peak. However, since the calculated total decays for this peak is lower than the value for most of the other peaks, and since the background count rate is so low, the effect of the background peak are minimal in this situation. The total number of decays of is 3848±81.

**<sup>52</sup>V**

Energy	Measured Energy (keV)	Counts	Relative Intensities (%)	Calculated Total Decays (x100)	Background Peaks?	Count Rate (per hour)
1434.06	1434.59	52 ± 7	0.47569	109.5 ± 15.8	No	0
1333.62		Not Detected	0.003		No	0

**Table A9:** <sup>52</sup>V spectrum observations

Since <sup>52</sup>V is practically monochromatic, not much needs to be said.

## The Unidentified

Sample	Start Energy	End Energy	Sigma	Counts
187W	1592.45	1594.1	3.6485	42.47 ± 11.64
198Au	156.13	157.23	3.5132	231.35 ± 65.85
198Au	244.91	246.55	3.6341	225.73 ± 62.11
198Au	249.84	250.93	3.5176	188.12 ± 53.48
198Au	602.21	603.85	3.6617	102.62 ± 28.02
198Au	2102.1	2104.84	3.5946	47.72 ± 13.28

**Table A10:** Possibly significant but unidentified peaks

This table contains all the identified peaks where  $\sigma > 3.5$ . If my statistical analysis was slightly optimistic, or effected by nearby peaks, then perhaps this  $\sigma$  value is too high. In this case, it is possible that some, or all, of these peaks are false positives.